Effects of CdCl2 treatment on deep levels in CdTe and their implications on thin film solar cells; A comprehensive photoluminescence study

DHARMADASA, I <http://orcid.org/0000-0001-7988-669X>, ECHUNDU, O.K., FAUZI, F., ABDUL-MANAF, N.A., SALIM, H.I., DRUFFEL, T., DHARMADASA, R. and LAVEY, B.

Effects of $CdCl_2$ treatment on deep levels in CdTe and their implications on thin film solar cells; A comprehensive photoluminescence study

I. M. Dharmadasa**, O. K. Echendu, F. Fauzi, N. A. Abdul-Manaf and H. I. Salim

Materials and Engineering Research Institute, Sheffield Hallam University, Sheffield S1 1WB, UK.

T. Druffel, R. Dharmadasa and B. Lavery

Conn Centre for Renewable Energy Research, University of Louisville, Louisville, Kentucky 40292, USA.

Abstract

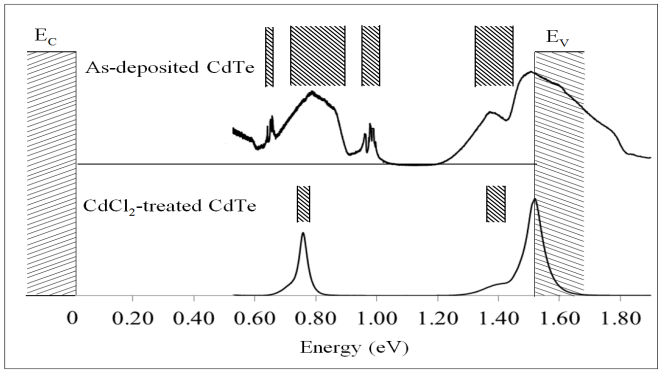

This work is aimed at studying defect level distributions in the bandgap of CdTe thin films, used for solar cell development. In particular, the effects of $CdCl_2$ treatment on the defect levels are the main objectives of this research. Four different CdTe thin films were electroplated using three different Cd-precursors ($CdSO_4$, $Cd(NO_3)_2$ and $CdCl_2$), and bulk CdTe wafers purchased from industry (Eagle Pitcher and University Wafers in US) were studied using low temperature photoluminescence. The finger prints of defects, 0.55 eV below the conduction band down to the valence band edge were investigated. In all of the CdTe layers, four electron trap levels were observed with varying intensities but at very similar energy positions, indicating that the origin of these defects are mainly from native defects. $CdCl_2$ treatment and annealing eliminates two defect levels and the mid-gap recombination centres are reduced drastically by this processing step. The optical bandgap of all four as-deposited CdTe layers is ~1.50 eV, and reduces to ~1.47 eV after $CdCl_2$ treatment. The material grown using the $CdCl_2$ precursor seems to produce CdTe material with the cleanest bandgap, most probably due to the built-in $CdCl_2$ treatment while growing the material.

Keywords; CdTe, Electroplating, $CdCl_2$ treatment, Photoluminescence, Defects in semiconductors

---

**Corresponding Author, E-mail: Dharme@shu.ac.uk, Tel: +44 114 225 6910 Fax: +44 114 225 6930

1.0 Introduction

Thin film solar cells based on CdS/CdTe structures have achieved 21% efficiency to date, for small area, lab-scale solar cells [1]. The performance, reproducibility, yield, stability and lifetime of these solar cells depend on defect levels present in the materials and device structures. Therefore, a thorough knowledge of these defect levels is of paramount importance in the research, development and manufacturing of CdS/CdTe solar panels to achieve higher efficiencies.

The heat treatment of CdTe thin films in the presence of $CdCl_2$ is a key processing step for achieving high performance devices. Although this treatment has been used over the past three decades, full understanding has not been achieved yet and this processing step requires careful research in some key areas. The defects signature in thin film CdTe has been identified as one of these key areas for careful investigation, in a recent comprehensive review [2], and this is the main subject of this publication.

This work presents photoluminescence (PL) studies carried out at 80 K on four different electroplated CdTe layers using three Cd-precursors. In this research programme, CdTe layers were electroplated using aqueous solutions of $CdSO_4$ [3], $Cd(NO_3)_2$ [4] and $CdCl_2$ [5] as the Cd-precursors, and TeO_2 solution as the Te-precursor. PL of these materials was studied to investigate the defects "finger prints"; thereby enabling the best performing Cd precursor to be selected for the electro-deposition of CdTe for photovoltaic applications. In the three cases described above, the CdTe was electroplated using a graphite anode; while in the fourth case, CdTe was grown using a platinum anode. The PL was used to examine the defects structure in the bandgap of the four different CdTe thin films, and the results are compared with the PL spectra observed for two different bulk CdTe wafers purchased from industry.

2.0 Experimental

The CdTe layers used were electrodeposited on glass/FTO/CdS substrates using aqueous solutions containing Cd-precursor and TeO_2 solution. Two of the four different CdTe layers used in this work were grown using $CdSO_4$ precursor with two different anodes (Pt and graphite) [3]. The other two CdTe layers were grown using $Cd(NO_3)_2$ precursor [4] and $CdCl_2$ precursor [5] both with graphite anode as reported in recent publications. The chloride precursor was used in a 3-electrode system, with saturated calomel as the reference electrode, while the other precursors were used in 2-electrode systems. All Cd-precursors used were purchased from Fisher Scientific and the purity was 99%. The solutions were electro-purified for ~100 hrs before deposition of CdTe layers. The concentration of the Cd-precursor in all cases was 1.0 M. pH value was at 2.00±0.02 at the start of the growth and temperature was raised to 85ºC for the 2-electrode system, and to 70ºC for 3-electrode system. A dilute TeO_2 solution was added to the electrolyte at regular intervals in order to maintain a low level of Te in the bath. The four electroplated CdTe layers were grown by four different researchers using different chemicals and various growth parameters. Hence, these layers can be considered as different CdTe materials. The main aim of this work is to examine the defect

structure present within the bandgaps of these materials, and to decide which Cd-precursor produces the best CdTe layers for fabricating CdS/CdTe thin film solar cells. The second aim was to explore the effects on defect levels when heat treated in the presence of $CdCl_2$. The final aim was to explore the effects of electroplating CdTe using a $CdCl_2$ solution, where the precursor will introduce a built-in $CdCl_2$ treatment during the growth.

In order to compare the finger prints of the defects existing in thin film CdTe layers, together with that of melt-grown bulk CdTe, PL studies were also carried out on CdTe wafers purchased from industry (University Wafers). Dimensions of these wafers were typically (10×10×1) mm^3 and one surface was polished to a mirror finish with 0.5 microns size diamond paste. This paper also re-visits the PL results obtained in the past for CdTe wafers purchased from Eagle Pitcher, to compare with present results on thin film CdTe layers.

Photoluminescence work was carried out using a Renishaw inVia Raman Microscope with a 632 nm (~1.96 eV) He-Ne laser as the excitation source. The detector used in this system is a combination of a diffraction grating and a CCD camera. The system is capable of measuring a wide range of energies. The samples were cooled to approximately 80 K using a Linkam THMS600/720 temperature controlled stage with liquid nitrogen and maintained at this temperature over the length of the PL measurement. The PL peaks in the energy range, 0.55 and 1.85 eV below the conduction band (CB) were explored in order to investigate any differences of defect levels and the band-to-band electron transitions.

After measuring the PL spectra of the as-deposited layers, $CdCl_2$ treatment was carried out in two steps. The first step was by treating the samples in ~1% $CdCl_2$ aqueous solution and heat treating at 440ºC for 8 minutes. The second step was carried out by treating the surface again with ~1% $CdCl_2$ aqueous solution and heat treating at 440ºC for 16 minutes. The aim here is to examine the trend in changes of defect levels existing in the forbidden gap of CdTe during this processing step.

3.0 Results and Discussion

The photoluminescence process can be understood by referring to the electron excitation and subsequent transitions taking place from the CB to defects and the valence band (VB), as shown in Figure 1. When the CdTe surface is excited by laser light of 632 nm (1.96 eV), electrons are continuously pumped from VB to the CB. These electrons are then captured by electron traps (T_n), as they make the transition from the CB towards the VB, therefore emitting photons with different energies in order to create various PL peaks. Band-to-band electron transitions create a peak providing the energy gap of the material. In order to produce PL peaks, traps should be electron traps with high concentrations and large cross-sections, and the transitions must be radiative. In this PL set-up, only the electron trap levels, ~0.55 eV below the CB can be observed down to the VB edge due to the limitations of the detector system used.

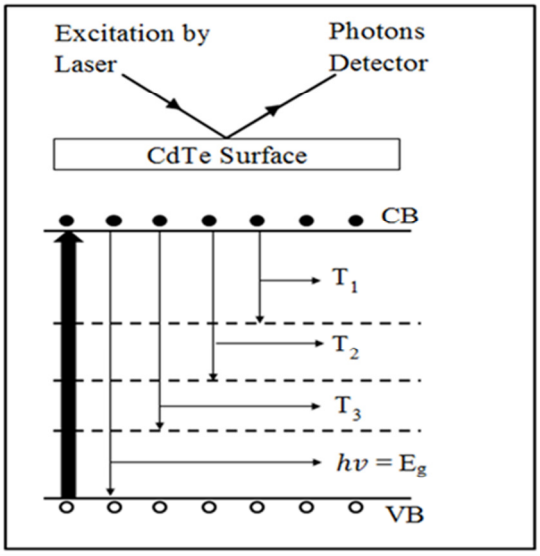

Figure 1. Schematic diagram showing the excitation of electrons from the valence band to the conduction band and subsequent electron trapping due to defects in the bandgap as the electrons make transitions from the conduction band towards the valence band.

3.1 Photoluminescence observations from thin films of CdTe

Typical PL spectra recorded at 80 K for the thin film CdTe layers grown from different precursors are shown in Figure 2. Five main PL peaks labelled T_1 - T_4 and E_g can be observed in the energy range, 0.55 eV to 1.85 eV as summarised in Table 1. The energy values corresponding to the maxima of these peaks are given in Table 1 together with their approximate energy spread. The peak positions at 80 K can be converted into room temperature values when necessary, using the rate of change of energy bandgap, $(dE_g/dT) = -4.2\times10^{-4}$ eVK^{-1} as reported for CdTe [6]. The maxima of the peaks appear at 0.66, 0.79, 0.97, 1.37 and 1.50 eV at 80 K, indicating at least four deep defect levels situated in the explored energy range, below the conduction band minimum. The peak at 1.50 eV corresponds to the energy bandgap of CdTe showing band-to-band electron transitions. The trap levels T_1, T_3 and T_4 are narrow, but the electron traps at 0.79 eV (T_2) spread over ±0.15 eV wide energy range. It is noteworthy that T_2 is a widely distributed defect and situated right in the middle of the bandgap. Therefore, these defects are very effective in recombination process, causing detrimental effects in PV performance. These defects kill photo-generated charge carriers through recombination and hence known as "killer centres" in II-VI semiconductors. A good solar energy material should be free of these mid-gap killer centres.

It should be noted that the joining of two PL spectra in these measurements is taking place on the T_3 level. Therefore, the observation of a clear peak at T_3 is disturbed, but this feature can be observed in all PL spectra. However, the identification of a peak at 0.97 eV is not that difficult from these measurements on four different layers.

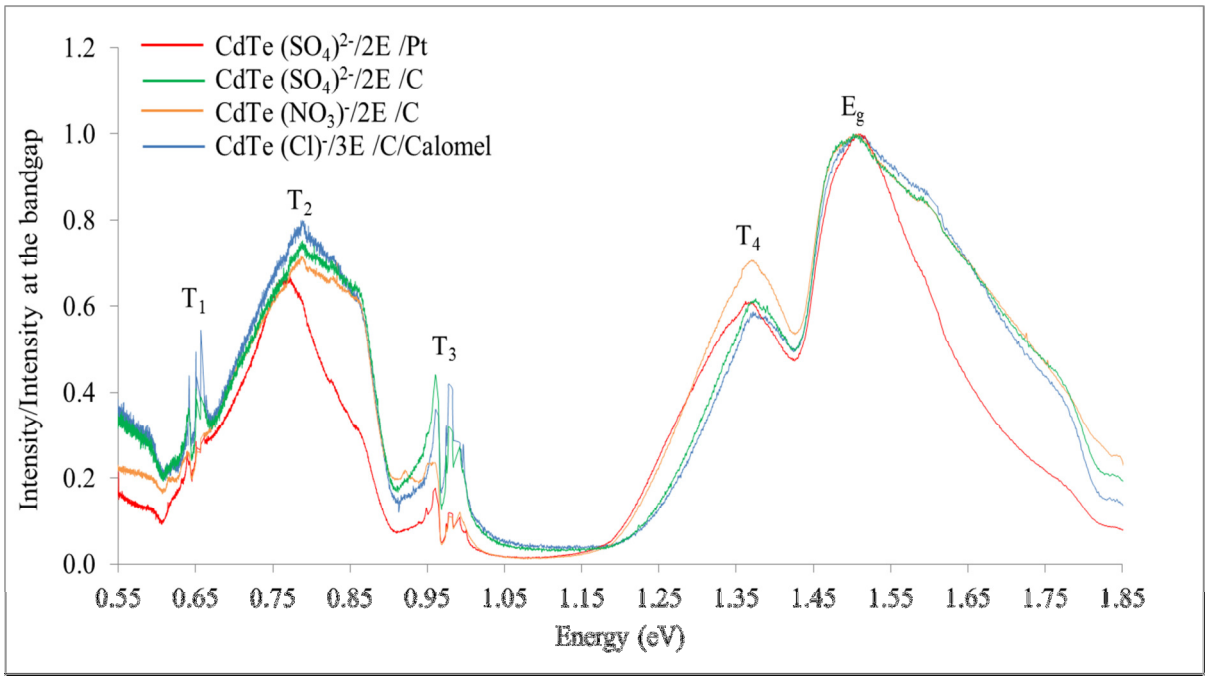

Figure 2. Typical photoluminescence spectra recorded at 80 K for four as-deposited CdTe layers using different Cd-precursors (sulphate, nitrate and chloride). The intensity of peaks are normalised to that of the band-gap emissions.

Table 1. Summary of electron trap levels (T_1,…T_4) and the energy bandgap (E_g) observed at 80 K for the four as-deposited CdTe layers. 2E and 3E stands for 2-electrode and conventional 3-electrode systems respectively. Pt and C shows the material used for anode.

Energy (eV)	T_1±0.02	T_2±0.15	T_3±0.03	T_4±0.08	E_g
CdTe (SO_4^{2-})/2E/Pt	0.66	0.77	0.97	1.36	1.51
CdTe (SO_4^{2-})/2E/C	0.66	0.79	0.97	1.37	1.50
CdTe (NO_3^-)/2E/C	0.66	0.79	0.98	1.37	1.50
CdTe (Cl^-)/3E/C	0.66	0.79	0.98	1.37	1.50

Although the defect level, T_4 also has a broader distribution, the probability of recombination through this level is very low due to its closeness to the valence band. The peak showing the band-to-band transition is also broad and extends beyond the bandgap of CdTe. The emissions greater than E_g may arise due to quantum effects and the presence of $CdS_xTe_{(1-x)}$ alloy at CdS/CdTe interface. The electroplated CdTe material consisting of grains in nano-scale could exhibit quantum effects in electron transitions creating photons greater than the bandgap. The emissions less than E_g can arise due to donor-to-acceptor type transitions, involving shallow energy levels, within the bandgap.

Figure 3 shows the PL spectra recorded for the CdTe layer electroplated using $CdSO_4$ precursor and 2-electrode system with Pt anode. The three spectra correspond to the as-deposited and $CdCl_2$ treated CdTe in two steps. The observed peak details are summarised in Table 2, and a few major changes are clear from these results. The two defect levels at T_1 and

T_3 completely disappear during $CdCl_2$ treatment. The broad distribution of T_2 narrows down and T_4 level reduces indicating drastic removal of defects from the bandgap. The value of bandgap reduces from 1.51 eV to 1.47 eV after $CdCl_2$ treatment, indicating the coalescence of small crystallites into large CdTe grains. This removes the quantum effects and therefore reduces larger values for E_g transitions.

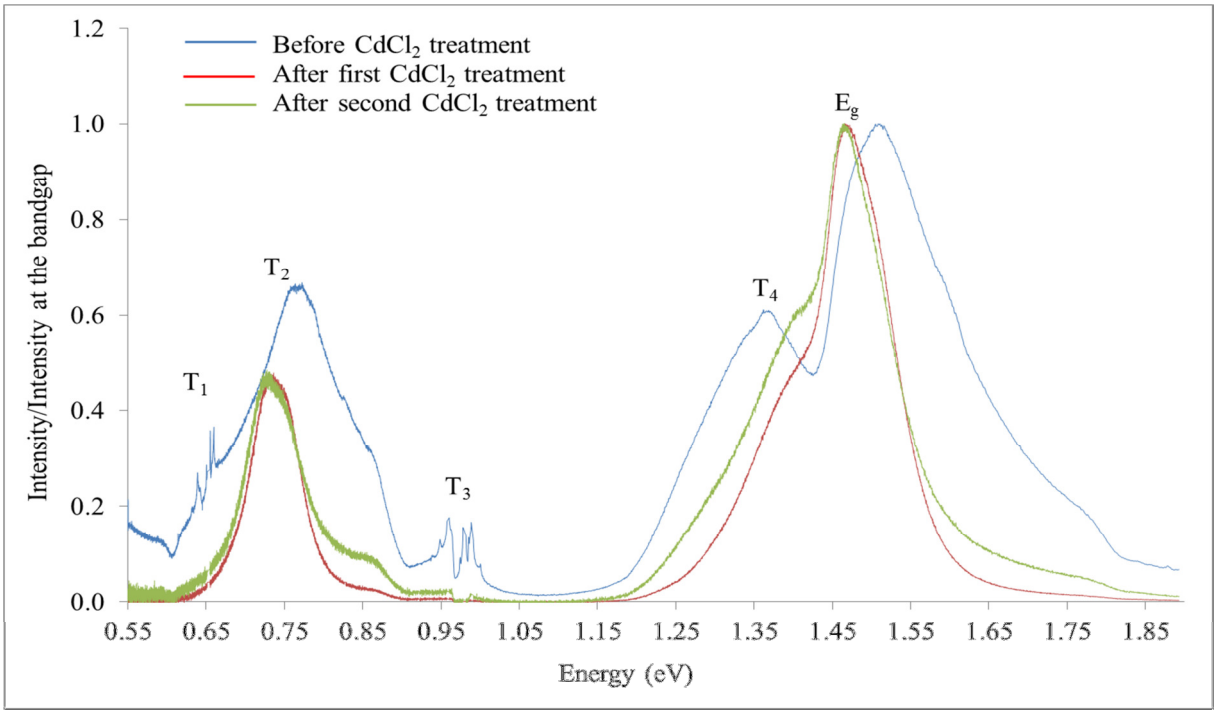

Figure 3. Photoluminescence spectra for as-deposited, first $CdCl_2$ treated and second $CdCl_2$-treated CdTe layers, electroplated using $CdSO_4$ precursor in 2-electrode system with Pt anode.

Table 2. Summary of electron traps at 80 K for CdTe layers electroplated from $CdSO_4$ precursor using 2-electrode system with Pt anode.

Energy (eV)	T_1	T_2	T_3	T_4	E_g
As deposited	0.66	0.77	0.97	1.36	1.51
$CdCl_2$-Step 1	-	0.73	-	1.39	1.47
$CdCl_2$-Step 2	-	0.73	-	1.39	1.47

Figure 4 and Table 3 show the PL spectra and details of defects for the CdTe layer grown from $CdSO_4$ precursor using 2-electrode system with graphite (C) anode. The same four defect levels are observed, and the disappearance of T_1 is clear after $CdCl_2$ treatment. Reduction of T_3 is evident but the defects are not completely removed. Although the intensities of T_2 and T_4 peaks have gone down, the distribution has not reduced. Clearly, the layers are full of defects even after $CdCl_2$ treatment and these will have detrimental effects on device performance. It should be noted that each of the four layers under study was electroplated by a different researcher introducing various differences. At the same time, these layers are not yet fully optimised to achieve high efficiency devices.

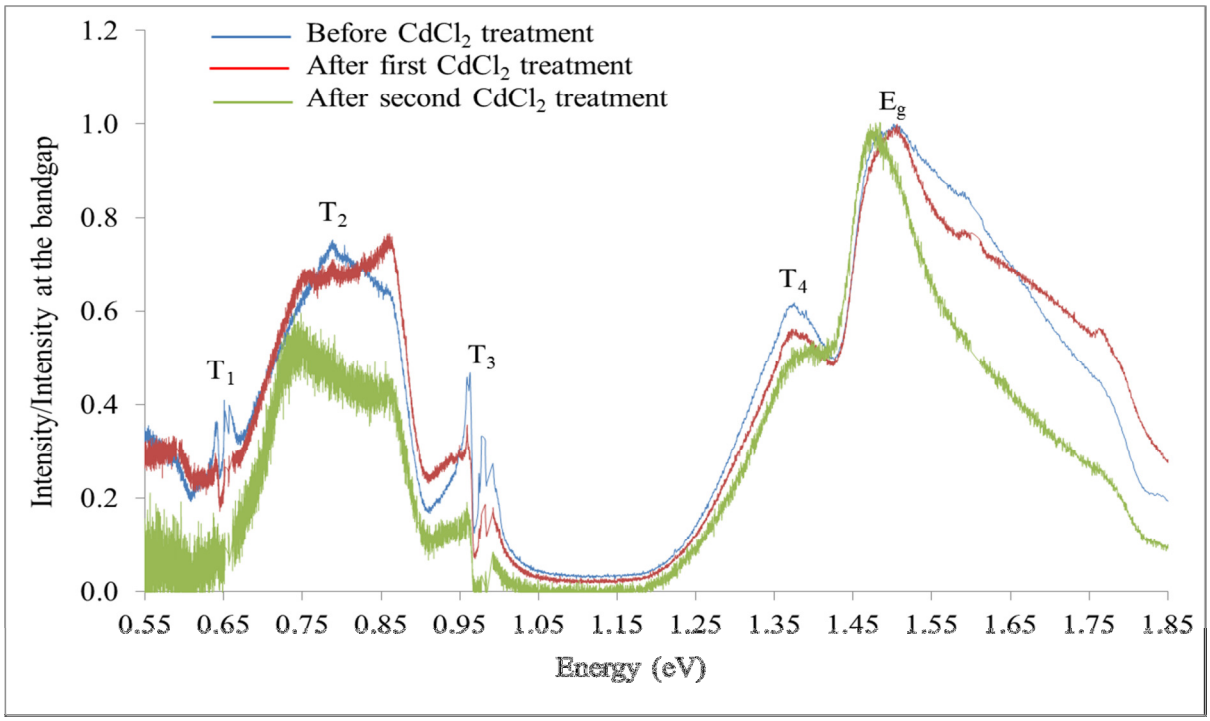

Figure 4. Photoluminescence spectra for as-deposited, first $CdCl_2$ treated and second $CdCl_2$-treated CdTe layers electroplated using $CdSO_4$ precursor in 2-electrode system with graphite anode.

Table 3. Summary of electron traps at 80 K for CdTe layers electroplated from $CdSO_4$ precursor using 2-electrode system with graphite anode.

Energy (eV)	T_1	T_2	T_3	T_4	E_g
CdTe - As deposited	0.66	0.79	0.97	1.37	1.50
CdTe - $CdCl_2$-Step 1	-	0.76	0.97	1.37	1.50
CdTe - $CdCl_2$-Step 2	-	0.74	0.97	1.38	1.48

Figure 5 and Table 4 present the PL spectra and the peak details for CdTe layers grown with $Cd(NO_3)_2$ precursor, using a 2-electrode system with graphite anode. The most striking observation is that the peak positions are in general very similar for all the CdTe layers. After $CdCl_2$ treatment, T_1 completely disappears and, T_3 peak still remains in this case. Although the intensity of T_2 has reduced considerably, the distribution remains the same. Intensity of T_4 first reduces and then increases with addition of more $CdCl_2$ to the treatment. The band-to-band emission peak sharpens by reducing the width of the peak. The bandgap of 1.50 eV for as-made layer reduces to 1.48 eV after $CdCl_2$ treatment.

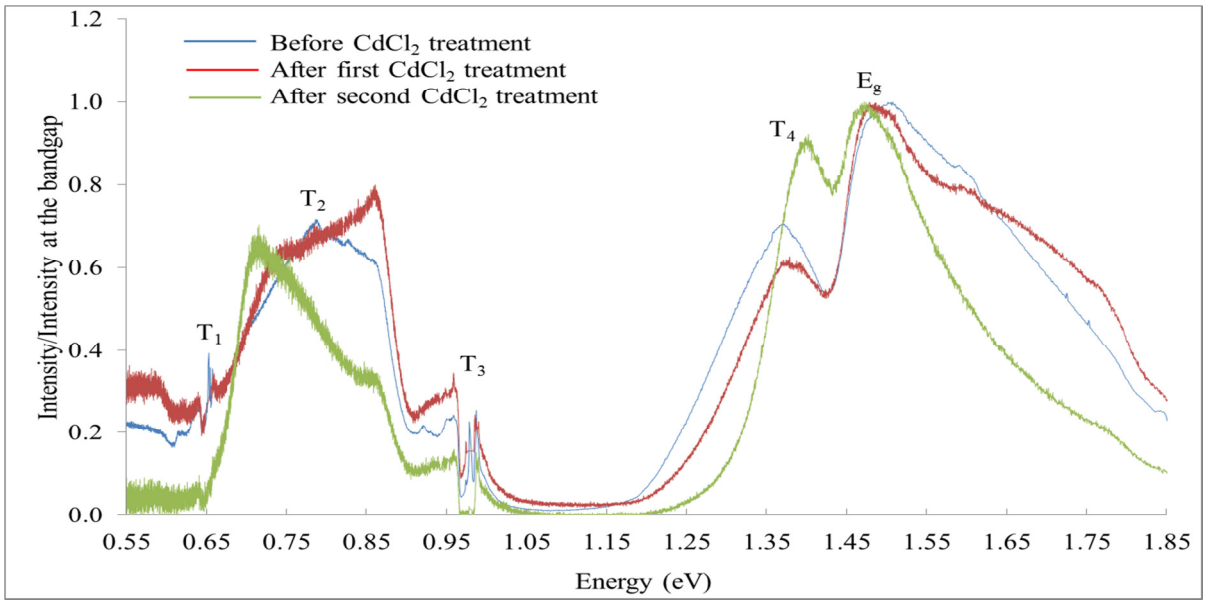

Figure 5. Photoluminescence spectra for as-deposited, first $CdCl_2$-treated and second $CdCl_2$-treated CdTe layers electroplated, using $Cd(NO_3)_2$ precursor in 2-electrode system with graphite anode.

Table 4. Details of PL peaks at 80 K for CdTe layers electroplated using $Cd(NO_3)_2$ precursor and 2-electrode system with graphite anode.

Energy (eV)	T_1	T_2	T_3	T_4	E_g
CdTe - As deposited	0.66	0.79	0.98	1.37	1.50
CdTe - $CdCl_2$-Step 1	0.66	0.86	0.99	1.38	1.48
CdTe - $CdCl_2$-Step 2	-	0.71	0.99	1.40	1.48

Figure 6 and Table 5 show similar results for CdTe layers grown using $CdCl_2$ precursor, in a 3-electrode system with a graphite anode. A saturated calomel electrode was used as the reference electrode in this system since Hg is not detrimental to CdTe based solar cells [7]. These layers provide well-defined PL spectra with most accurate peak positions. All five peaks in the as-deposited layer are identical in energy position terms to those of CdTe grown from other precursors, but show drastic changes after $CdCl_2$ treatment. The T_1 and T_3 defect levels are completely annealed-out during the $CdCl_2$ treatment. Considerable reduction of the energy distribution of T_2 from ~0.34 eV to ~0.09 eV is extremely important to note. Drastic reduction of the intensity of T_4 and sharpening of the bandgap peak are excellent results to observe. In particular, the drastic reduction of mid-gap "killer centres" at T_2 is good news for photovoltaic devices. It should be noted that the main difference in this layer is the electroplating from $CdCl_2$ precursor. Therefore the built-in $CdCl_2$ treatment is already there, even during the materials growth by depositing molecule by molecule. Therefore the effect of $CdCl_2$ treatment should be highest in this material. Changes at the band-to-band transitions are drastic and noteworthy. Formation of highly crystalline CdTe with low defects, in the presence of Cl^{-1} is clear from these results. It seems that Cl^{-1} are acting as a fluxing agent for growing CdTe with large crystals with low defects.

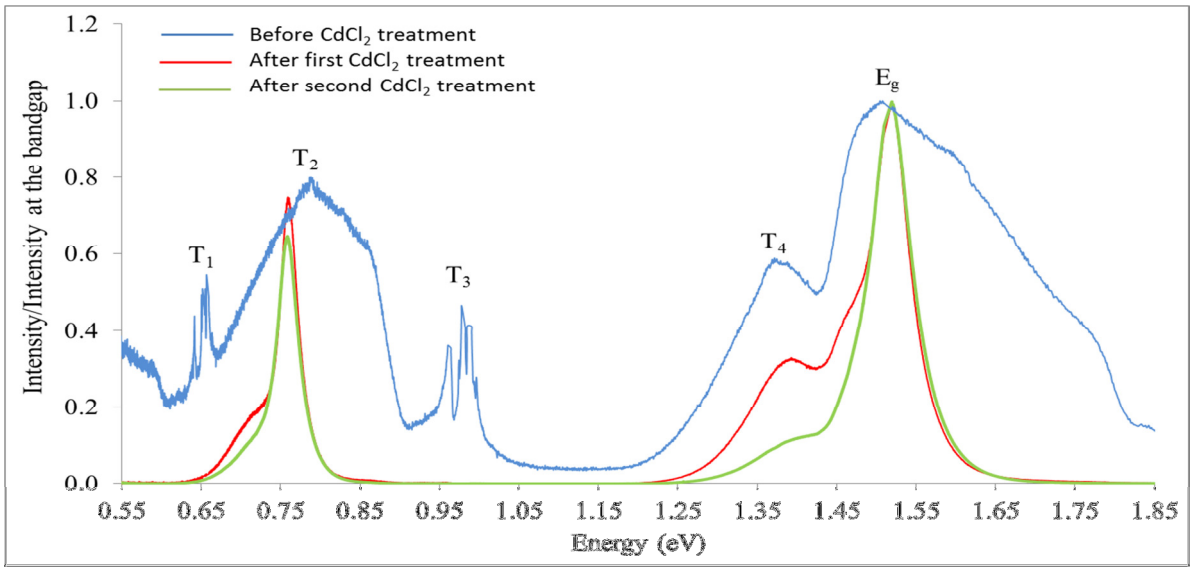

Figure 6. Photoluminescence spectra for as-deposited, first $CdCl_2$-treated and second $CdCl_2$-treated CdTe layers electroplated using $CdCl_2$ precursor and 3-electrode system with carbon anode and saturated calomel reference electrode.

Table 5. Details of PL peaks at 80 K for CdTe layers electroplated using $CdCl_2$ precursor and 3-electrode system with graphite anode and saturated calomel reference electrode.

Energy (eV)	T_1	T_2	T_3	T_4	E_g
As deposited	0.66	0.79	0.98	1.37	1.50
$CdCl_2$-Step 1	-	0.76	-	1.39	1.51
$CdCl_2$-Step 2	-	0.76	-	1.39	1.51

A summary of PL studies on all four CdTe layers are given in Table 6. Trap levels for both as-deposited and $CdCl_2$ treated (after second stage) samples are shown for comparison. Four trap levels have been observed for all CdTe layers in the explored energy range. T_2 situated at the mid-gap is a broad peak spreading over ~0.30 eV, and will be more effective in recombination of photo-generated charge carriers created during PV action under illumination.

Table 6. Summary of observed PL peaks at 80 K for four different CdTe layers electroplated from three different Cd-precursors (sulphate, nitrate and chloride).

Growth details	Material condition	T_1 (eV)	T_2 (eV)	T_3 (eV)	T_4 (eV)	E_g (eV)
CdTe-(SO_4^{2-})/2E/Pt	As-Deposited	0.66	0.77	0.97	1.36	1.51
	$CdCl_2$ treated	----	0.73	----	1.39	1.47
CdTe-(SO_4^{2-})/2E/C	As-Deposited	0.66	0.79	0.97	1.37	1.50
	$CdCl_2$ treated	----	0.74	0.97	1.38	1.48
CdTe-(NO_3^-)/2E/C	As-Deposited	0.66	0.79	0.98	1.37	1.50
	$CdCl_2$ treated	----	0.71	0.99	1.40	1.48
CdTe-(Cl^-)/3E/C	As-Deposited	0.66	0.79	0.98	1.37	1.50
	$CdCl_2$ treated	----	0.76	----	1.39	1.51

When heat treated in the presence of $CdCl_2$, T_1 and T_3 completely reduce in some samples, but in others show a considerable reduction. T_2 is the main defects band presence at right in the middle of the bandgap and distributed in a wide energy range of ~0.30 eV. These are the most detrimental defects for PV action, with the highest probability of recombination process. T_4 appears at 1.39 eV, with varying intensity after $CdCl_2$ treatment. Therefore, as graphically shown in Figure 7, $CdCl_2$ treatment helps in removing defects and clearing the bandgap of CdTe.

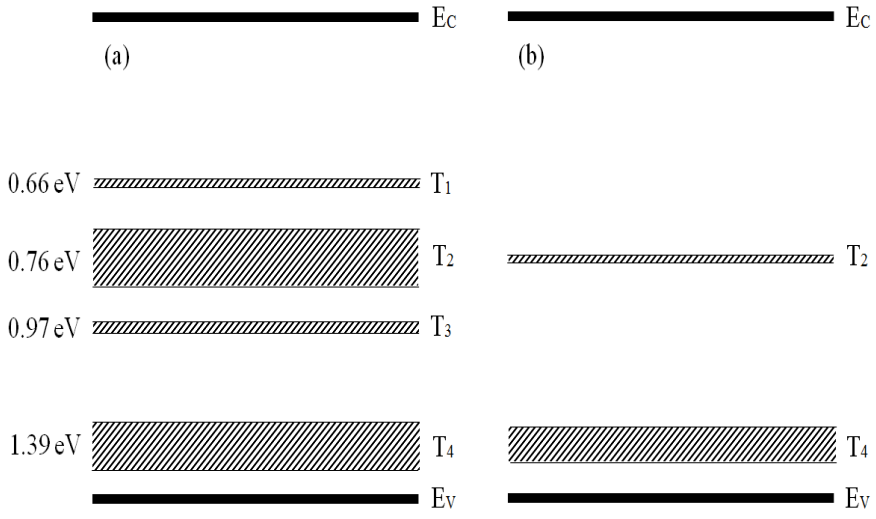

Figure 7. A graphical summary of defects finger-print observed at 80 K for (a) as-deposited and (b) $CdCl_2$ treated thin films of CdTe grown by electroplating.

The bandgap of as-deposited layers is ~1.50 eV at 80 K. After $CdCl_2$ treatment, this value reduces to ~1.47 eV, except for the sample grown in $CdCl_2$ precursor, which remains at 1.50 eV. The 1.50 eV bandgap at 80 K corresponds to 1.41 eV at room temperature, which agrees well with the bandgap of bulk CdTe.

3.2 Photoluminescence observations from bulk CdTe material

3.2.1 Bulk CdTe from University Wafers

In order to compare the PL results of thin films of CdTe with bulk material, (10×10×1) mm^3 wafers were purchased from University Wafers in the United States and the PL measurements were carried out under similar conditions, on polished surfaces. In order to observe any useful changes on the surface, these wafers were also treated with $CdCl_2$ and heat treated at 440°C for 20 minutes. The surface was then rinsed well with de-ionised water and the PL spectrum was recorded at 80 K in the same measurement system.

Figure 8 shows the PL spectra recorded for polished CdTe wafer before and after $CdCl_2$ treatment. As-received material shows two sharp peaks corresponding to 0.76 eV (T_2) mid-gap defects and 1.52 eV (E_g) energy gap of the material. These are identical to the two peaks, T_2 and E_g observed for thin films of CdTe. After $CdCl_2$ treatment, T_2 level shows slight broadening and additional peak at 1.39 eV (T_4) appears, showing that these changes are due

to $CdCl_2$ inducement on the surface layer. A review [24] by Fernández on PL and CL results also summarize the increase of this particular level upon $CdCl_2$ treatment. This information is extremely important in understanding what happens during this key processing step. The conclusion is that this additional defect level, T_4 emerges due to Cd-richness or the incorporation of Cl in CdTe. This PL observation is also very similar to cathodoluminescence (CL) work reported by Mazzamuto et al [8]. These authors reported the development of this peak at 1.39 eV when Freon ($CHFCl_2$) gas pressure in the heating chamber is gradually increased during the heat treatment of close space sublimation (CSS) grown CdTe thin films. Since there are no additional Cd involved in this treatment, Cd-richness can be eliminated with confidence. This provides us a firm conclusion of the origin of this defect at 1.39 eV (T_4), below the CB edge. Cl interacts with CdTe lattice forming a defect level at 1.39 eV, very close to the VB. This level therefore, can act as a shallow acceptor in CdTe increasing the acceptor concentration (N_A) within the material. This information is helpful in understanding Cl as an amphoteric dopant. At ppm level, when Cl displaces Te atoms in the lattice, it is a well-known donor in CdTe [9]. However, when Cl concentration is high as in the case of $CdCl_2$ treatment, and interacts with CdTe layer, it produces an acceptor like defect at 1.39 eV (T_4), acting as a p-type dopant in CdTe. Interaction of Cl within CdTe layer is not-known at present, and need extra information to draw firm conclusions. The final electrical conductivity type depends on the resultant value of (N_D - N_A) in the material. This value can also depend on heat treatment temperature and the duration.

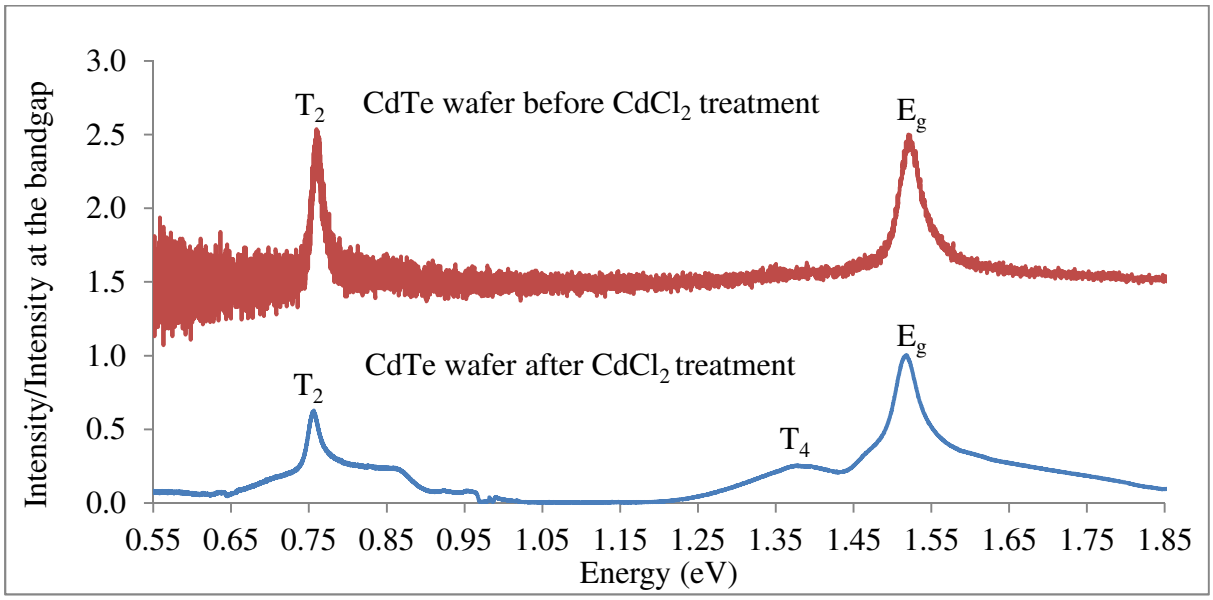

Figure 8. Photoluminescence spectra recorded before and after $CdCl_2$ treatment, for bulk CdTe wafers purchased from University Wafers. These wafers were produced using a melt-growth technique and the dimensions of the wafers used were (10×10×1) mm^3.

It is really striking to see the similarity of PL spectra of commercially available CdTe bulk materials with electroplated CdTe thin films using $CdCl_2$ precursor, after $CdCl_2$ treatment. These two spectra are plotted in Figure 9 for direct comparison. It is clear that the thin film CdTe layers of the order of 1.0 µm can be grown with comparable defect levels in the bulk CdTe bandgap.

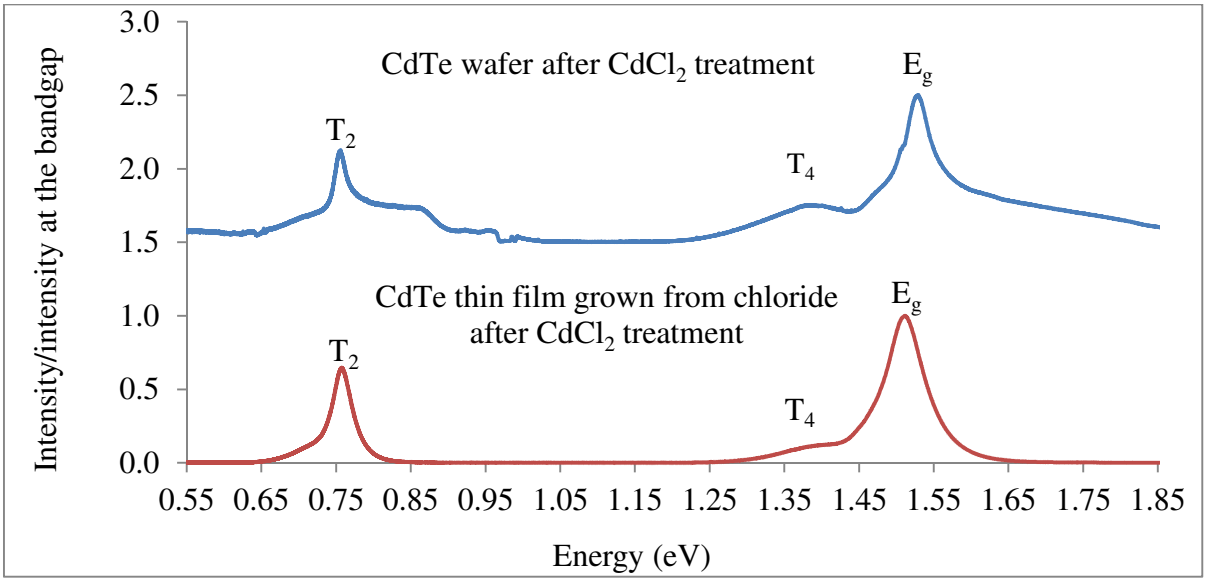

Figure 9. Photoluminescence spectra of bulk CdTe wafers and electroplated CdTe thin films from chlorides, after $CdCl_2$ heat treatment. Note the cleaner bandgap in the $CdCl_2$ treated thin film CdTe grown using $CdCl_2$ precursor, with a built-in $CdCl_2$ treatment.

3.2.2 Bulk CdTe from Eagle Pitcher

It is also worth re-visiting the PL measurements carried out on bulk CdTe wafers purchased from Eagle Pitcher, in the past by the main author [10]. Figure 10 shows the PL spectra obtained at 4 K, together with corresponding X-ray photo-electron spectra (XPS) of the surfaces investigated. The CdTe surfaces were mechanically polished and chemically etched to produce Te-rich or Cd-rich surface layers, and the PL spectra were recorded under same experimental conditions. The Te-richness and Cd-richness were confirmed using XPS experiments carried out on these surfaces [11].

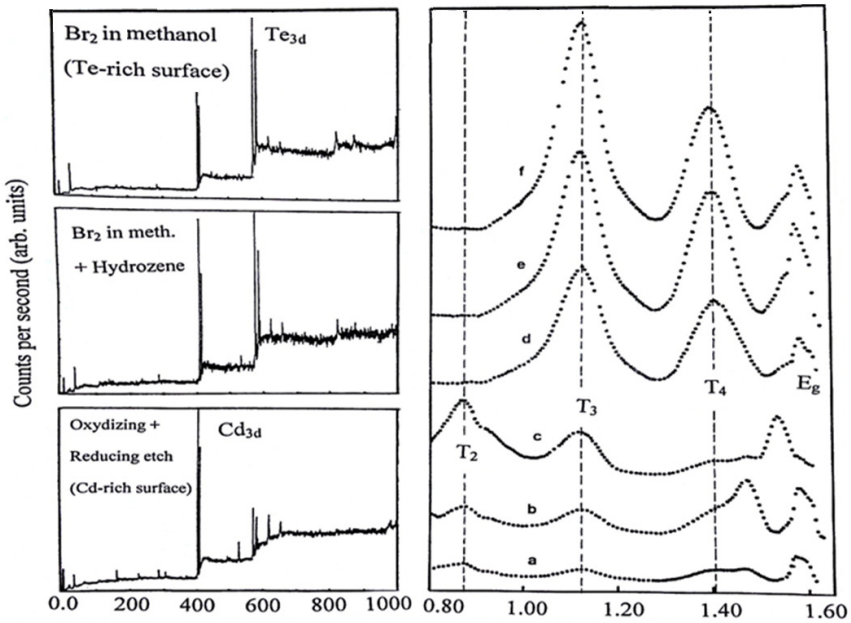

Figure 10. The XPS spectra [11] of Te-rich and Cd-rich CdTe surfaces and their corresponding PL spectra obtained at 4 K [10]. The CdTe wafers were purchased from Eagle Pitcher in United States. The spectra (a, b & c) corresponds to PL from Te-rich surfaces and (d, e & f) corresponds to PL from Cd-rich surfaces. Note the observation of four peaks, T_2, T_3, T_4 and E_g with very similar energies observed for thin films of CdTe.

Figure 10 shows the defect levels observed by purposely modifying the CdTe surfaces by chemical etching. The energy values can be converted to 80 K for comparison using the rate of change of the bandgap given in section 3.1. The main defect levels observed at 80 K for bulk materials and the CdTe thin films grown using $CdCl_2$ precursor are summarised in Table 7. The results presented in this paper shows that defects present in CdTe are common for at least six different CdTe materials produced with different conditions. The heat treatment in the presence of $CdCl_2$ turn the material into electronic grade layers with only two or three deep defect levels present in them. The most important results observed from Figure 10 are that, T_2 is dominant for Te-rich layers and T_3 and T_4 are dominant for Cd-rich CdTe layers. This provides us a method to control deep levels in CdTe material.

Table 7: Summary of defect levels observed from PL, for bulk CdTe from University Wafers, and Eagle Pitcher, and for thin film CdTe layers grown using $CdCl_2$ precursor and after $CdCl_2$ treatment.

Material	T_2 (eV)	T_3 (eV)	T_4 (eV)	E_g (eV)
Bulk CdTe (University Wafers)	0.76		1.39	1.52
Bulk CdTe (Eagle Pitcher)	0.84	1.09	1.37	1.52
Thin Films of CdTe grown by $CdCl_2$ precursor after $CdCl_2$ treatment	0.76		1.39	1.51

4.0 Implications of deep defect levels on CdTe based solar cells

4.1 Effects on Materials

It is now worth looking at the summary of PL results observed for both thin films and bulk CdTe materials. It is evident that there are at least four main discrete defect levels existing in the bandgap of CdTe. It is a striking result to observe deep level defects at very similar energy values (see Tables 6 and 7) for four different thin films grown differently using various Cd-precursors and for two different bulk CdTe material grown at two commercial companies. This means that these defects must be arising from native defects in CdTe.

The observations of Figure 10 for chemically etched bulk CdTe surfaces show that the intensities of defects related peaks are much higher than that of the bandgap peak. This means that the electron transitions from E_c to defects are much stronger than E_c to E_v. In opto-electronic device applications, these types of transitions are not very useful. However, the peak intensities shown in Figure 6 and Table 8 for CdTe thin films grown using $CdCl_2$ precursor show that the E_g peak is much higher than the defect related peaks. This is the feature necessary for solar energy materials to fabricate efficient solar cells. A material with low intensity defect peaks will produce better devices. The counts of E_g peak for as-deposited

material has increased from 8143 to 514,331 after the second $CdCl_2$ treatment. This clearly shows that defects in the bandgap have drastically annealed-out and the band-to-band transitions have increased. This is the main reason that the $CdCl_2$ treatment is essential in order to fabricate efficient CdTe solar cells.

Table 8. Intensity of band-to-band electron transitions (E_g peak) for CdTe thin films grown using $CdCl_2$ precursor, and after $CdCl_2$ treatment.

CdTe $(Cl)^-$ 3E/C	E_g peak intensity (Photon counts)
As-deposited	8,143
$CdCl_2$ treated – step 1	60,740
$CdCl_2$ treated – step 2	514,331

Observations in Figure 10 also help in drawing another important conclusion. In Te-rich surfaces, defects (T_2) in the mid-bandgap are dominant, and in Cd-rich surfaces, defects in lower half of the bandgap (T_3 and T_4) are dominant. This observation is also confirmed by the $CdCl_2$ treatment of thin film CdTe layers presented in this paper. Results summarised in Table 6 and Figure 7 clearly show that $CdCl_2$ treatment removes the trap levels at T_1 and T_3, and drastically reduce the wide distribution of T_2 to a narrow distribution level. These are the defect levels situated towards the middle of the bandgap and related to the Te-richness of CdTe materials. Out of the two elements, Cd and Te in CdTe, Te is the easiest element to discharge first and deposit during electroplating (E^o for Te is +0.593 V, and E^o for Cd is -0.403 V). Therefore Te can be precipitated [12-14] within the layer or form a thin layer of Cd_xTeO_y on the surface [15]. Hence, most of the as-deposited CdTe layers have Te-rich nature and therefore T_1, T_2 and T_3 trap levels are dominant. However, when these layers are heat treated in the presence of $CdCl_2$ on the surface, excess Te converts into useful CdTe phase improving the stoichiometry of the CdTe layer.

$$\text{Excess Te} + CdCl_2 \longrightarrow CdTe + Cl^-$$

The presence of Cl^- in this process also helps in recrystallisation and doping of the CdTe. In fact, the $CdCl_2$ treatment converts Te-richness of the initial CdTe layer into Cd-richness, reducing defects at T_1 and T_2. This produces a CdTe layer with fairly clean bandgap removing defects in the mid-gap (see Figure 7). The same process increases the band-to-band transitions of electrons, as a result of removal of mid-gap defect levels (see Table 8) producing a better solar energy material.

4.2 Effects on Devices

At this point, re-visiting the electrical contact work published in the past [11, 16-18], showing preparation of Cd-rich and Te-rich CdTe surfaces leading to form different Schottky barriers at metal/n-CdTe interfaces is highly relevant. Figure 11 shows I-V characteristics of Schottky diodes produced by metal/n-CdTe interfaces. The barrier heights are independent of the metal used, and the same metal (Sb, Au, etc.) produces low barriers (~0.72 eV) on Te-rich surfaces and high barriers (~0.96 eV) on Cd-rich surfaces. In these cases, the Fermi level pins at T_2 for

Te-rich surfaces and at T_3 for Cd-rich CdTe surfaces. It is obvious that once the defects at T_1, T_2 and T_3 are removed from the bandgap, extremely large Schottky barriers can be produced by pinning the FL at T_4 (~1.26 eV at room temperature). This is indeed routinely observed in our CdTe devices made out of electrodeposited Cd-rich CdTe layers [15].

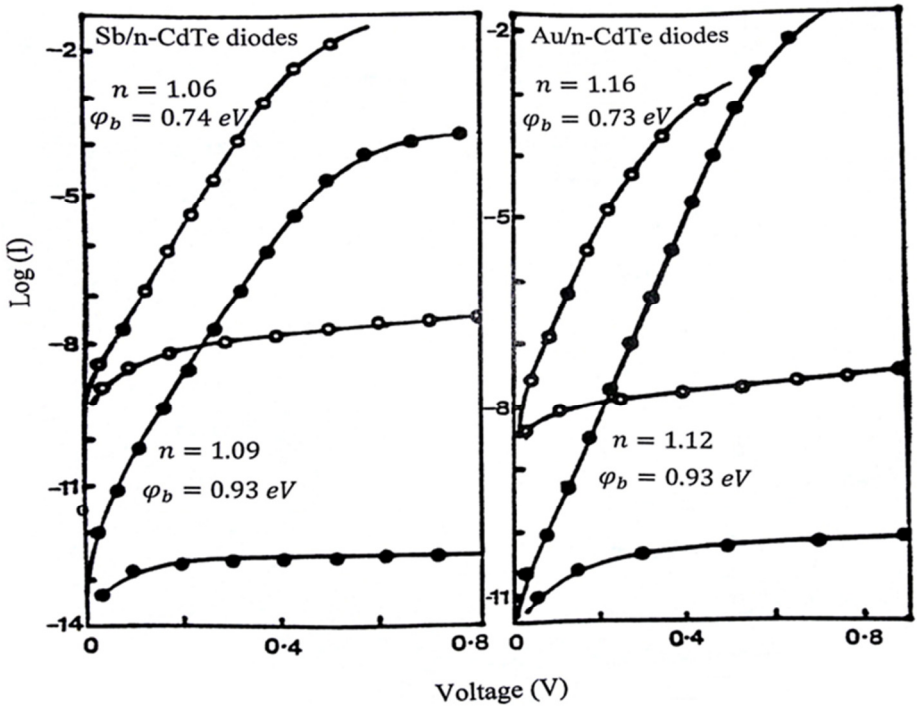

Figure 11. Typical Schottky diode characteristics produced on Te-rich and Cd-rich CdTe wafers (Eagle Pitcher) with Sb and Au electrical contacts. Barrier heights are independent of the metal used and create due to strong FL pinning positions at T_2 level when Te-rich and at T_3 levels when Cd-rich [11, 17-19].

The most striking effect is the observation of similar discrete barriers for thin film CdTe layers [17]. From the results presented in this paper, it is clear that the defect levels in CdTe are common at least for six different materials and play a very important role in Schottky barrier formation at metal/n-CdTe interface. This Fermi level pinning affects the performance of CdTe based solar cells as published before [11, 16-18]. Pinning the Fermi level at the defect level at T_3 (~0.92 eV room temperature) or at T_4 (~1.24 eV at room temperature) produces high potential barriers at metal/n-CdTe interfaces creating excellent rectification properties exceeding ~10^8 rectification factors at 1.0 V.

The most recent ultra-violet photoemission spectroscopy (UPS) work [19] on electroplated CdTe thin films confirmed that the Fermi level settles in the upper-half of the bandgap after $CdCl_2$ treatment. This means that under $CdCl_2$ treatment, N_D remains greater than N_A and hence the material remains n-type after $CdCl_2$ treatment. It is also extremely important to note Schulmeyer et al's work on CSS-CdTe layers obtained from Antek [20]. These authors performed XPS studies on $CdCl_2$ treated CSS-CdTe layers and determined the position of the FL in CdTe, and measured the efficiency of fully fabricated CdS/CdTe device structures.

They reported that the highest efficiencies are observed when the FL is ~0.85 eV above the VB. This means that the FL has settled ~0.60 eV below the conduction band minimum, and material remained n-type after $CdCl_2$ treatment. Their work also confirms the production of highest efficiency values when devices are fabricated with CSS grown n-type CdTe layers.

In order to make high performing solar cells, one needs to grow high quality n-type CdTe layers without defects at T_1, T_2 and T_3. The material should have high concentrations of T_4 defects influenced by $CdCl_2$ treatment, in order to pin the FL at the vicinity of T_4 level (~1.26 eV at room temperature). Combining all the results presented in this paper and the most useful and relevant information published in the literature, the energy band diagram of the most efficient CdS/CdTe solar cell is shown in Figure 12. As at present, the mid-gap T_2 defect related to Te-richness is still present in the CdTe bandgap. Complete removal of T_1, T_2 and T_3 and pinning the FL at the T_4 defect level will produce high performing devices reducing recombination process. This FL pinning can be enhanced by adding p-dopants such as Cu, Sb, As, Bi, etc. to the electrical contact material. Also by adding p-type and wide bandgap semiconducting layers such as p-ZnTe and p-type organic polymers on CdTe, the FL can be forced to keep very close to the VB of CdTe. Φ_b at the back contact can be further improved using MIS-type electrical contacts forming barrier heights exceeding the energy gap of CdTe. This will lead to production of large V_{oc} values for this solar cell. This device architecture as proposed in 2002 [17, 18], is a tandem device of an n-n hetero-junction in the front connected in parallel to a large Schottky barrier at the back. In this parallel connection, CB is connected to CB, instead of connecting the CB to the VB in series connection or tunnel-junction approach [21]. In this device structure with parallel connection of the two junctions, V_{oc} remains constant and the current density (J_{sc}) adds up from two devices. MIS type electrical contacts could produce barrier heights greater than the bandgap of CdTe and hence produce high V_{oc} values also.

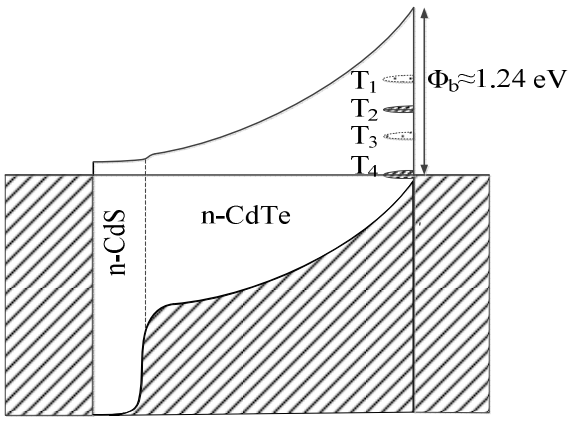

Figure 12. Energy band diagram of CdS/CdTe solar cell depicting four main deep levels observed using PL studies carried out in this work. The Fermi level is pinned at T_4 level.

Since CdTe can be easily produced either in p-type or n-type electrical conduction, there exists two types of device structures; genuine single p-n junctions, and combined two junctions as shown in Figure 12. Highest efficiencies are produced by the two-junction devices, but all interpretations in the past were given in terms of a simple p-n junction. This

has created a severe confusion in the CdS/CdTe development field and hence stagnated the conversion efficiency ~16% [22, 23] for over two decades. Proper understanding of the materials and device issues, designing and developing the appropriate device architectures, optimising the materials growth and device processing steps will lead to produce high performing CdS/CdTe solar cells with efficiencies well above the current values of 21% in the near future.

5.0 Conclusions

The photoluminescence results presented in this paper and other highly relevant information from the literature leads to draw following important conclusions.

(a) All four CdTe layers electroplated using sulphate, nitrate and chloride of cadmium precursors exhibit four electron traps (T_1, T_2, T_3 and T_4) situated at similar energy positions. The bulk CdTe wafers purchased from Eagle Pitcher and etched surfaces also exhibit three defects at T_2, T_3 and T_4. Materials from University Wafers show only one defect level at T_2 in the mid-gap.

(b) When compared with PL intensities of the electroplated materials with the chemically etched bulk material surface, band-to-band transitions are strong in thin film CdTe layers. This indicates the low-trap concentrations in electroplated materials after $CdCl_2$ treatment.

(c) After $CdCl_2$ treatment, T_1, T_2 and T_3 completely anneal-out or show considerable reduction in concentration. This reduction is a positive effect for device performance.

(d) $CdCl_2$ treatment drastically reduces the mid-gap killer centres situated at T_2 level. Wide distribution (~0.30 eV) reduces to a narrow defect band (~0.09 eV) and the intensity also reduces by considerable amounts. This will have a drastic and positive effect on improvement of solar cell performance by reducing recombination of photo-generated charge carriers.

(e) The two defect levels T_1 & T_2, situated in the mid-gap are closely related to Te-richness in CdTe layers. $CdCl_2$ treatment converts the Te-richness towards Cd-richness, reducing precipitated Te, drastically removing mid-gap defects.

(f) Out of all four CdTe layers studied in this work, the material grown using $CdCl_2$ precursor seems to produce a better material with a cleaner bandgap. This material is comparable to University Wafers - CdTe in terms of defect levels. The built-in $CdCl_2$ treatment during the growth of the layer may be the most possible reason. However, it should be noted that all these layers are grown by four different researchers and are not grown at optimised conditions.

(g) All CdTe layers seem to have the defect level at T_4, and $CdCl_2$ treatment seems to enhance this defect. Fermi level pinning at T_3 (~0.92 eV at RT) or at T_4 (~1.26 eV at RT) produce large Schottky barrier at n-CdTe/metal interface and hence produce high performing

CdS/CdTe solar cells. The most desirable level to pin the FL is ~1.26 eV below the conduction band.

Acknowledgements

Authors would like to thank and acknowledge the contributions made by Paul Bingham, Mohammed Madugu, Olajide Olusola and Ayothunde Ojo, through technical discussions.

5.0 References

[1] First Solar Builds the Highest Efficiency Thin Film PV Cell on Record, Press Release on 5 August 2014, http://investor.firstsolar.com/releasedetail.cfm?ReleaseID=864426

[2] Review of the $CdCl_2$ Treatment Used in CdS/CdTe Thin Film Solar Cell Development and New Evidence Towards Improved Understanding, Dharmadasa I.M., Coatings 2014, 4(2), pp282-307; doi:10.3390/coatings4020282.

[3] Optimisation of CdTe electrodeposition voltage for development of CdS/CdTe solar cells, Diso D.G., Fauzi F., Echendu O.K. and Dharmadasa I.M., Submitted to Coatings October 2014.

[4] Electrodeposition of CdTe thin films solar cells using nitrate precursor, Salim H.I., Patel V., Abbas A., Walls M. and Dharmadasa I.M., Submitted to Journal of Materials; Materials for Electronics, in April 2014.

[5] Abdul-Manaf N. A. et al, un-published experimental results.

[6] Tsay Y.F., Mitra S.S. and Vetelino J.F., J. Phys. Chem. Solids, 34 (1973) p 2167.

[7] Dharmadasa I.M. et al, un-published experimental results.

[8] Mazzamuto S., Vailant L., Bosio A., Romeo N., Armani N., Salviati G., A study of the CdTe treatment with a Freon gas such as CHF_2Cl. Thin Solid Films 2008, 16, 7079–7083.

[9] Zanio K., Semiconductors and Semimetals, Volume 13, Cadmium Telluride: Academic Press, New York, NY, USA, 1978.

[10] Correlation of Photoluminescence measurements with the composition and electronic properties of chemically etched CdTe surfaces. Sobiesierski Z., Dharmadasa I.M. and Williams R.H., Appl. Phys. Lett. 1988, 53(26) pp2623-2625.

[11] Effects of surface treatments on Schottky barrier formation at metal/n-CdTe contacts. Dharmadasa I.M., Thornton J.M. and Williams R.H., Appl. Phys. Lett. 1989, 54(2) p137.

[12] Ayoub M., Hage-Ali M., Zumbiehl A., Regal R., Koebel J.M., Rit C., Fougères P. and Siffert P., IEEE Transactions on nuclear science, Vol.49, No.4 (2002) pp1954-1959.

[13] Bugár M., Belas E., Grill R., Procházka J., Uxa S., Hlidek P., Franc J., Fesh R. and Höschl P., IEEE Transactions on nuclear science, Vol. 58, No.4 (2011) pp1942-1948.

[14] Ayoub M., Hage-Ali M., Koebel J.M., Zumbiehl A., Klotz F., Rit C., Regal R., Fougères P. and Siffert P., IEEE Transactions on nuclear science, Vol. 50, No.2 (2003) pp229-237.

[15] High short-circuit current density CdTe solar cells using all-electrodeposited semiconductors, Echendu O.K., Fauzi F., Weerasinghe A.R. and Dharmadasa I.M., Thin Solid Films 556 (2014) 529-534. doi: 10.1016/j.tsf.2014.01.071.

[16] Recent developments and progress on electrical contacts to CdTe, CdS and ZnSe with special reference to barrier contacts to CdTe. Dharmadasa I.M., Invited review paper. Progress in Crystal Growth and Characterisation. Vol. 36, No. 4. (1998) pp 249-290.

[17] New ways of development of Glass/Conducting Glass/CdS/CdTe/metal thin film solar cells based on a new model. Dharmadasa I.M., Samantilleke A.P., Young J. and Chaure N.B., Semicond. Sci. Technol. 17 (2002) pp1238-1248.

[18] Advances in Thin Film Solar Cells. (2013) Dharmadasa I.M., A single authored book, Pan Stanford Publishing Ltd., Singapore.

[19] Study of Fermi level movement during $CdCl_2$ treatment of CdTe thin films using Ultra-violet Photoemission Spectroscopy, Dharmadasa I.M., Echendu O.K., Fauzi F., Salim H. I. and Abdul-Manaf N.A., Jasinski J.B., Sherehiy A. and Sumanasekera G., Submitted to Chemistry and Physics of Materials, September 2014.

[20] Schulmeyer T., Fritsche J., Thiβen A., Klein A., Jaegermann W., Campo M. and Beier J., Effect of in situ UHV CdCl2-activation on the electronic properties of CdTe thin film solar cells, Thin Solid Films 431 – 432 (2003) 84 – 89.

[21] Third Generation Multi-layer Tandem Solar Cells for Achieving High Conversion Efficiencies, Dharmadasa I.M., Solar Energy Materials & Solar Cells, 85 (2005) pp293-300.

[22] Britt J. and Ferekides C., Thin Film CdS/CdTe Solar cell with 15.8% Efficiency, Appl. Phys. Lett. 62 (1993) 2851 - 2852.

[23] Wu X., Keane J.C., Dhere R.G., DeHart C., Albin D.S., Duda A., Gessert T.A., Ashar S., Levi D.H. and Sheldon P., 16.5%-efficient CdS/CdTe polycrystalline thin film solar cells. In: Proceedings of 17th European PVSEC (2001) 995-1000.

[24] Fernández P., Defect structure and luminescence properties of CdTe based compounds, Journal of Optoelectronics and Advanced Materials, Vol. 5, No. 2 (2003) 369-388.